Journal of Materials Science: Materials in Electronics (2021) 32:12746–12757
https://doi.org/10.1007/s10854-020-03473-w

REVIEW

Review on applications of PEDOTs and PEDOT:PSS in perovskite solar cells

Yijie Xia[1] · Shuyang Dai[1]

Received: 12 March 2020 / Revised: 10 April 2020 / Accepted: 25 April 2020 / Published online: 5 May 2020

Abstract

Poly(3,4-ethylenedioxythiophene):poly(styrene sulfonate) (PEDOT:PSS) is the most successful conducting polymer in terms of practical application. It has good film forming ability, high transparency in visible light range, high mechanical flexibility, high electrical conductivity, and good stability in air. PEDOT:PSS has wide applications in many areas. This review summarizes its new applications in perovskite solar cells and approaches to modify the PEDOT:PSS layer for better device performance with the corresponding mechanisms. The most cutting edge progresses in perovskite solar cells with PEDOT:PSS are highlighted.

1 Introduction

Poly(3,4-ethylenedioxythiophene):poly(styrene sulfonate) (PEDOT:PSS, chemical structure is shown in Fig. 1) is a polymer electrolyte consisting of positively charged conjugated PEDOT and negatively charged insulating PSS. Oxidized PEDOT is highly conductive but is insoluble in water. PSS is a polymer surfactant, which facilitates PEDOT to stably disperse in water and other solvents. The PEDOT:PSS aqueous dispersion is commercially available. It was first commercialized under the trade name of Baytron® by Bayer AG, then by H. C. Starck, and currently by Heraeus under the trade name of Clevios™, and Orgacon™ by Agfa [1, 2]. Among them, the less-conductive PEDOT:PSS aqueous solution like Clevios P VP a.i. 4083 [3–8] is widely used to create hole transport/injection layers in optoelectronic devices, and highly conductive PEDOT:PSS solutions including Clevios PH500 [9, 10] and Clevios PH1000 [11–15] are usually applied to fabricate highly conductive and flexible electrodes.

High-quality PEDOT:PSS films can be readily formed using the PEDOT:PSS aqueous dispersion through conventional solution-processing techniques, such as spin casting, slot die coating, doctor blade, spray deposition, screen printing, inkjet printing, etc. The PEDOT:PSS film is normally uniform and smooth (roughness < 5 nm). PEDOT:PSS thin film is highly transparent in the visible light range. For example, the transmittance (T) of a 100-nm-thick PEDOT:PSS film is higher than 90% at 550 nm. The electrical conductivity of PEDOT:PSS film can be tuned from 10^{-2} to 10^{3} S/cm through the control of synthetic conditions, the use of different additives or post-treatment methods [12, 16–31]. The work function of PEDOT:PSS film is 5.0-5.2 eV, that is favored for charge injection and transfer with fast kinetics thus providing PEDOT:PSS with catalytic properties. Furthermore, PEDOT:PSS possesses high mechanical flexibility, excellent thermal stability and low cost. Therefore, PEDOT:PSS or PEDOT have been widely used in photovoltaics (PVs), displays, transistors and various sensors [32–47]. These applications and the approaches of the electrical conductivity enhancement of PEDOT:PSS have been reviewed [48–54].

Nowadays, PEDOT:PSS has new applications in perovskite solar cells (PSCs). Since the first solid-state perovskite solar cell has been developed with a remarkable power conversion efficiency (PCE) of 9.7% by Kim et al. in 2012 [55], PSCs have attracted a lot of research interest in recent years because of their low fabrication cost and very impressive energy conversion efficiency [56–81]. The PCE of PSCs has been elevated to 24.2%, which is comparable to silicon solar cell [82]. The high energy conversion efficiency is related to the appropriate bandgap, high charge carrier mobility, long carrier diffusion length, efficient free charge carrier generation and broadband absorption of perovskite materials [83,

✉ Yijie Xia
xiayj@usst.edu.cn

[1] School of Mechanical Engineering, University of Shanghai for Science and Technology, Shanghai 200093, People's Republic of China

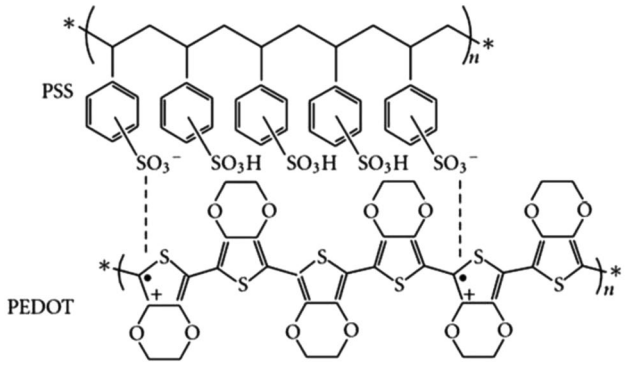

Fig. 1 Chemical structure of PEDOT:PSS

71, 84–88]. It has been reported that optimization of the perovskite layer can achieve high PCE [89–94]. And the electrical conductivity, surface morphology and work function of the hole transport layer (HTL) can also affect the performance of PSCs [95–101].

In this review, we present a snapshot of the applications of PEDOT:PSS and PEDOT as HTL or electrode in perovskite solar cells. We mainly focus on the approaches to enhance the PEDOT:PSS and device performances, as well as the corresponding mechanisms of the performance enhancements. The most cutting edge progresses in perovskite solar cells with PEDOT:PSS are highlighted.

2 PEDOT:PSS as a hole transport layer in perovskite solar cells

Due to its high transparency in visible light range, good film forming property via solution processes, as well as intrinsically high work function, PEDOT:PSS was traditionally used as a hole injection and transport layer in organic light-emitting diodes and organic solar cells. Nowadays, since PSCs gain a lot of research interest, PEDOT:PSS naturally becomes a popular HTL in inverted PSCs. The properties of PEDOT:PSS layer can affect the PSCs' performance. First, there is an energy gap between PEDOT:PSS (− 5.12 eV) and $CH_3NH_3PbI_3$ (− 5.4 eV) perovskites, resulting in relatively low open circuit voltages (V_{oc}, < 1 V). Thus, the V_{oc} of PSCs can be improved by increasing the energy level of PEDOT:PSS. In addition, the electrical conductivity of as-prepared PEDOT:PSS films from aqueous PEDOT:PSS solution is usually below 1 S/cm, which is lower than that of common metal cathode. Such interior conductivity of PEDOT:PSS layer leads to the energy loss during the process of charge carrier transport, thereby decreasing the photocurrent, fill-factor (FF) and the PCEs of PSCs [102–106]. Thus, it is important to enhance the conductivity of PEDOT:PSS. Furthermore, the gradient of the electrical conductivity near the surface area to bulk and microstructure defects in PEDOT:PSS film morphology can lead to an inefficient hole transfer inside the PEDOT:PSS layer [107–109], causing an unbalanced carrier charge transport and the accumulation of charge carrier, and ultimately results in low FF and large leakage of current [110–113]. Thus, the uniformity of PEDOT:PSS layer is important to the PSCs' performance.

Many attentions have been paid to the modification of the PEDOT:PSS layer for PSCs' performance improvement [114–142, 105, 143]. Table 1 summarizes the works using PEDOT:PSS as HTL in PSCs' application. Generally, there are four kinds of methods to improve the electrical and optical properties of PEDOT:PSS film: post-treatment, doping, composite and bilayer.

2.1 Post-treatment

It has been reported that the properties of PEDOT:PSS film, including conductivity, morphology and work function, can be improved by post-treatment. Many efforts have been made to improve the performance of devices through post-treatment.

Most studies primarily focused on solvent treatment of PEDOT:PSS layer, since solvent treatment can improve the conductivity and surface morphology of PEDOT:PSS. For instance, Ouyang group [30] investigated the post-treatment of perovskite precursor solutions on PEDOT:PSS film. The solution deposition of perovskite materials can significantly enhance the conductivity of PEDOT:PSS layer, leading to an increased J_{sc} (short circuit current). Later, Bruijnaers et al. [129] showed that spin-coating of a precursor solution reduces the oxidation state of PEDOT:PSS. This reduction leads to a lowering of the work function of the PEDOT:PSS and the perovskite layer on top of it. Recently, Zhang et al. [122] studied the effect of polyethyleneglycol-200 (PEG-200) post-treatment on PEDOT:PSS layer. They found that the PEG-200 can not only greatly enhance the conductivity but also improve the morphology of PEDOT:PSS, leading to a better contact interface between PEDOT:PSS and perovskite layer. The conversion efficiency of the cells can be enhanced to 12.56%. Subsequently, Reza et al. [143] found that post solvent treatment of PEDTO:PSS film with ethylene glycol and methanol dramatically increased the conductivity and hydrophobicity of the film, resulting in formation of smooth and highly crystalline perovskite films with larger grains. This achievement of highly conductive HTL and efficient charge extraction with high-quality perovskite films led to a remarkable increase in device efficiency to 18.18% ± 0.40%.

Rather than solvent, inorganic materials were also applied to treat the PEDOT:PSS layer. Luo et al. [136] reported that spin-coating a graphene-oxide (GO) solution onto the PEDOT:PSS surface can remove the redundant PSS

Table 1 The performance of PSCs with PEDOT:PSS as HTL

Product	Method	Active layer	Area (mm^2)	V_{oc} (V)	J_{sc} (mA cm^{-2})	FF (%)	PCE (%)	Year	Ref.
N.A.	PEDOT:PSS/CuSCN composite	$CH_3NH_3PbI_3$/PCBM	9	1.02	19.10	78.52	15.30	2020	[114]
Clevios 4083	PEDOT:PSS/GQDs composite	$CH_3NH_3PbI_3$/PCBM	10	0.995	21.07	72.68	15.24	2019	[115]
Clevios 4083	Ethylene glycol and methanol treatment	$CH_3NH_3PbI_3$/PCBM	16	1.04	22.21	79	18.18	2019	[143]
Clevios 4083	PEDOT:PSS/SrGO bilayer	$CH_3NH_3PbI_3$/PCBM	N.A.	1.04	19.39	80.48	16.01	2019	[116]
Clevios P	PEDOT:PSS/WO_3 composite	$FA_{0.4}MA_{0.6}PbI_{2.8}Br_{0.2}$	4.5	1.03	22.69	64.84	15.10	2019	[117]
Clevios 4083	Ionic liquid doping	$CH_3NH_3PbI_3$/PCBM	8	1.08	23.81	78	20.06	2019	[118]
Clevios 4083	CTAB doping	$CH_3NH_3PbI_3$/PCBM	10	0.90	18.62	75	12.53	2019	[119]
Clevios 4083	Ammonia doping	$CH_3NH_3PbI_{3-x}Cl_x$/PCBM	4	0.95	20.73	68.7	13.51	2019	[120]
N.A.	Sodium citrate doping	$CH_3NH_3PbI_3$/PCBM	9	1.134	21.618	75.01	18.39	2019	[121]
Clevios 4083	PEG treatment	$CH_3NH_3PbI_3$/PCBM	6	0.79	23.02	61	12.56	2019	[122]
Clevios 4083	H_2O_2 oxidization	$CH_3NH_3PbI_{3-x}Cl_x$/PCBM	11	1.07	21.6	82	18.8	2019	[123]
Clevios 4083	Triton X-100 doping	$CH_3NH_3PbI_3$/PCBM	4	0.94	23.10	74.98	16.23	2019	[124]
Clevios P	PEDOT:spiro-OMeTAD composite	$Cs_{0.05}(FA_{0.83}MA_{0.17})_{0.95}Pb(I_{0.83}Br_{0.17})_3$	16	1.17	21.6	75.2	18.7	2019	[125]
Clevios 4083	RbCl doping	$MA_{0.7}FA_{0.3}Pb(I_{0.9}Br_{0.1})_3$/PCBM	11	1.00	22.41	82.41	18.30	2018	[76]
Clevios 4083	AMH doping	$CH_3NH_3PbI_3$/PCBM	4.5	0.910	21.68	74.06	14.61	2018	[126]
N.A.	Alanine doping	$Cs_xFA_{1-x}PbI_3$/PCBM	9	0.891	21.77	79.8	15.48	2018	[127]
N.A.	CuSCN treatment	$CH_3NH_3PbI_3$/PCBM	7	0.86	17.6	71.7	10.9	2018	[128]
Clevios 4083	Perovskite precursor treatment	$CH_3NH_3PbI_3$/PCBM	9	0.99	18.0	78	14.0	2018	[129]
Clevios 4083	CrO_3/PEDOT:PSS composite	$CH_3NH_3PbI_{3-x}Cl_x$/PCBM	7.25	0.98	22.83	76	16.90	2018	[130]
Clevios 4083	AuAg alloy nanocrystals doping	$CH_3NH_3PbI_{3-x}Cl_x$/PCBM	18.42	1.02	21.89	77.2	16.76	2018	[131]
Clevios 4083	Water rinsing treatment	$CH_3NH_3PbI_{3-x}Cl_x$/PCBM	11	1.11	20.11	80.6	18.0	2018	[77]
EDOT monomer	Dopamine-copolymerized PEDOT	$CH_3NH_3PbI_{3-x}Cl_x$/PCBM	7	0.96	19.69	71	13.42	2018	[132]
Clevios 4083	NaCl doping	$CH_3NH_3PbI_{3-x}Cl_x$/PCBM	11	1.08	20.5	81.9	18.1	2017	[78]
N.A.	Carbon black and DMSO doping	$CH_3NH_3PbI_3$/PCBM	N.A.	0.795	16.48	39.0	5.11	2017	[133]
Clevios 4083	DMSO doping	$CH_3NH_3PbI_3$/PCBM	1.8	0.92	22.76	80	16.7	2017	[134]
Clevios 4083	V_2O_5/PEDOT: PSS bilayer	$CH_3NH_3PbI_3$/PCBM	N.A.	0.884	22.69	74.70	15.0	2017	[135]
Clevios 4083	GO treatment	$CH_3NH_3PbI_3$/PCBM	N.A.	21.92	0.94	74.78	15.34	2017	[136]
Clevios 4083	SAF doping	$CH_3NH_3PbI_{3-x}Cl_x$/PCBM	7	1.02	20.25	68.0	14.05	2017	[71]
Clevios 4083	Ammonia doping	$CH_3NH_3PbI_{3-x}Cl_x$/PCBM	10	0.93	20.9	79.4	15.5	2017	[137]
Clevios 4083	PSSNa doping	$CH_3NH_3PbI_3$/PCBM	4	1.11	18.44	76.0	15.56	2017	[138]
Clevios PH1000	DMSO and Zonyl doping	$CH_3NH_3PbI_{3-x}Cl_x$/PCBM	17	0.97	17	75	12.5	2016	[141]
Clevios 4083	rGO/PEDOT:PSS composite	$CH_3NH_3PbI_3$/PCBM	13	0.95	17.1	64	10.6	2016	[140]

Table 1 (continued)

Product	Method	Active layer	Area (mm^2)	V_{oc} (V)	J_{sc} ($mA\ cm^{-2}$)	FF (%)	PCE (%)	Year	Ref.
Clevios 4083	PEDOT:PSS-GO-Glucose Nanocomposite	$CH_3NH_3PbI_3$/PCBM	4	1.05	17.6	69	12.8	2016	[141]
N.A.	TiO_2/MoO_3 NPs doping	$CH_3NH_3PbI_{3-x}Cl_x$/PCBM	7.92	0.96	17.35	84	13.63	2016	[142]
Clevios PH1000	PEO doping	$CH_3NH_3PbI_3$/PCBM	16	0.88	23.42	80.10	16.52	2016	[105]
Clevios 4083	MAI treatment	$CH_3NH_3PbI_{3-x}Cl_x$/PCBM	11	1.06	18.14	66	12.6	2015	[30]

component, improve wettability of PEDOT:PSS layer and inhibit the carrier recombination at the interface between the perovskite and PEDOT:PSS layers. Therefore, the cooperative interactions of these factors greatly improve the light absorption of the perovskite layer, the carrier transport and collection abilities of the PSCs, and especially the stability of the cells. Later, Xiong et al. [128] found that spin-coated inorganic CuSCN on PEDOT:PSS layer can change the energy states of PEDOT:PSS to decrease the energy loss during charge transport, promoting the charge transfer at the same time and forming good crystalline of perovskite film on CuSCN/PEDOT:PSS substrate. Based on the improved charge transport and reduced energy loss, the photovoltaic property of PSC based on CuSCN/PEDOT:PSS reaches the optimized efficiency of 10.9%.

New methods were developed to improve the PEDOT:PSS layer. Kuan Sun group [77] reported a facile method to construct PEDOT:PSS monolayers by water rinsing the spin-coated PEDOT:PSS films (Fig. 2). The PSCs with water-rinsed PEDOT:PSS as HTL yield improved PCE of 18.0%. The better device performance is ascribed to the internal electric field rooted from PEDOT/PSS bilayered structure that can facilitate better hole extraction. Moreover, the oriented arrangement of PEDOT:PSS monolayers endows higher work function and stronger hydrophobicity, leading to the enhancement in V_{oc} and stability in ambient environment. Later, they reported a facile two-step treatment [123]. The PEDTO:PSS layers were constructed by water rinsing followed by H_2O_2 oxidation. The oxidized PEDOT:PSS monolayer exhibited not only a high charge transfer efficiency to ensure faster hole extraction by the electrode but also a weak lateral charge movement. The device based on the H_2O_2-treated PEDOT:PSS monolayer showed a high FF of 82%, and a high PCE of 18.8%.

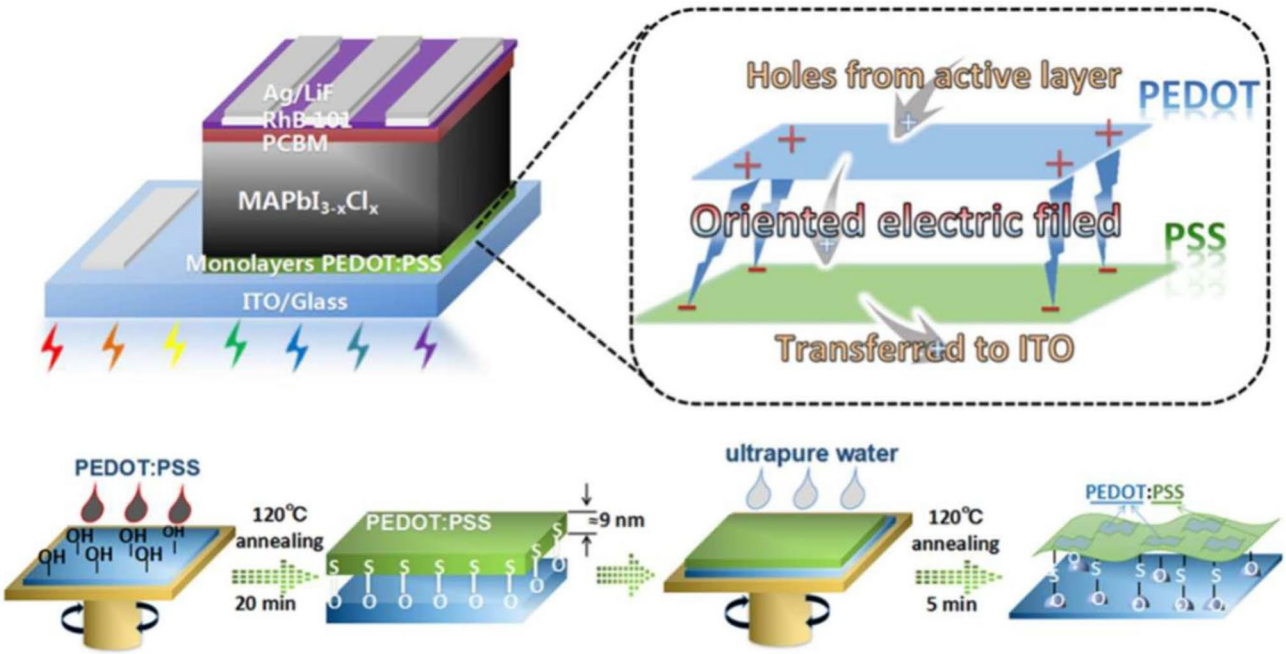

Fig. 2 Possible high efficiency working model of monolayers PEDOT:PSS film and briefly fabricated process [77]

2.2 Doping

Many research groups have improved the PCE of the devices by doping, which could adjust the conductivity, valence band, and acidity of PEDOT:PSS.

To prepare a more uniform perovskite film, ammonia and its compounds were doped with PEDOT:PSS to obtain a better perovskite film to achieve a higher FF and V_{oc}. Sun et al. [137] and Wang et al. [120] reported that PSCs using ammonia-modified PEDOT:PSS can obtain a PCE over 15%, which is attributed not only to the better energy-level alignment between the ammonia-modified PEDOT:PSS film and perovskite layer but also to the increased grain size and crystallinity of perovskite film. Subsequently, Zhu et al. [119] doped PEDOT:PSS with Cetyl trimethyl ammonium bromide (CTAB). The ammonium group in CTAB would passivate the bottom surface of perovskite film; Br^- in CTAB would diffuse into the perovskite film and exchange with iodide ion during the annealing process. As a result, PCE of the PSCs were increased to 12.53% with increased J_{sc} and V_{oc}. Fan et al. [126] introduced another ammonium compound, ammonium metatungstate hydrate (AMH), into PEDOT:PSS. The AMH-PEDOT:PSS HTL yields the perovskite with large average grain size, smooth and dense film. Consequently, the average PCE of 14.61% was achieved. Doping inorganic nanoparticles into PEDOT:PSS can also increase crystalline of the perovskite film with large-scale domains and a compact morphology. Liu et al. [142] mixed TiO_2/MoO_3 core/shell nanoparticles of approximately 40 nm with PEDOT:PSS layer to construct the HTL. The optimized device shows a high power conversion efficiency of 13.63%.

To engineer the electronic properties of PEDOT:PSS, Shin et al. [124] explored the effect of a nonionic surfactant, Triton X-100 (TX) additive. They found that the TX additive inhibits interface recombination between PEDOT:PSS and $MAPbI_3$, which is caused by the suppression of semimetallic properties of the PEDOT:PSS surface. The PCE of PSCs was increased to 16.23% with the TX-modified PEDOT:PSS. Li et al. [127] added alanine into pristine PEDOT:PSS, which was proved beneficial to reconstruct the distribution of the $–SO_3^-$ and $–SO_3H$ groups, resulting an improvement of the charge collection and transport owing to the weakened enrichment of $–SO_3H$. In this work, the initial power conversion efficiency (PCE) of 15.48% was achieved. It is known that the work functions of the charge transport materials affect the V_{oc} of perovskite solar cells significantly; thus researchers have improved the PCE of the devices through adjusting the valence band of PEDOT:PSS to match with perovskites and then enhanced the V_{oc} of the device. For instance, Zuo et al. [138] added polymer electrolyte sodium polystyrene sulfonate (PSS-Na) into PEDOT:PSS solution for performance enhancement and demonstrated an outstanding V_{oc} of 1.52 V. Metal nanocrystals had been used as the dopant into HTL or photoactive layers in organic solar cells to enhance the light harvesting by the scattering effect of metal nanocrystals. Sun et al. [131] applied AuAg core-shell alloy nanocrystals (ANCs) into PEDOT:PSS layer of PSCs as dopant for the first time. The devices based on AuAg ANCs-doped PEDOT:PSS reached a champion power conversion efficiency of 16.76%.

To increase the hole transport in PEDOT:PSS, Huang et al. [105] employed the highly electrical conductive polyethylene oxide (PEO)-doped PEDOT:PSS as the HTL for the PSCs. The dramatically enhanced electrical conductivity of the PEO-doped PEDOT:PSS HTL provides an efficient pathway for the hole extraction, transport, and collection from the perovskite active layer to the ITO anode. Other additives like DMSO [134], carbon black [133] and Zonxl [139] were used as dopant in PEDOT:PSS to increase conductivity and to enlarge the grain size of as-deposited perovskite thin film resulting in better stability. On the other hand, due to good chemical stability, negligible vapor pressure, high conductivity and low flammability, ionic liquids have also been applied to HTL in PSCs to enhance the efficiency via increasing the conductivity of hole transport film. Recently, Zhou et al. [118] found that doping of EMIC (1-ethyl-3-methylimidazolium chloride) ionic liquid can efficiently reduce the work function of the PEDOT:PSS HTL and improve the electronic conductivity and surface morphology of the PEDOT:PSS HTL in inverted PSCs. The PCE can be increased to 20.06%, which is the highest efficiency in the one-step PEDOT:PSS-based inverted PSCs so far.

To improve the performance of PEDOT:PSS film in other aspects, such as energy alignment, pH value, surface energy, and morphology, etc. at the same time, organic salt has been chosen as an additive due to its advantages like weak basicity, reducibility, etc. Recently, Hu et al. [121] reported a method of doping a commonly used nontoxic mild organic salt, sodium citrate, into PEDOT:PSS solution. The V_{oc} was impressively increased to 1.134 V and the PCE of the device was promoted to 18.39% accordingly. The higher work function of the doped PEDOT:PSS film and the uniform crystallinity of the perovskite film on it are regarded as the reasons for the increased V_{oc} and the consequent performance enhancement.

Sun et al. group found that doping inorganic salt into PEDOT:PSS solution can also significantly improve the PSCs' performance. They reported a method of doping PEDOT:PSS with soluble sodium salt (NaCl) with optimized PCE of more than 18.1% [78]. It is believed that an NaCl-doped PEDOT:PSS surface facilitates uniform nucleating perovskites and at the same time helps perovskite crystals orientate to get a uniform high-quality perovskite film. Subsequently, they doped dispersing rubidium chloride (RbCl) in the PEDOT:PSS aqueous solution [76] (Fig. 3). Based on systematic characterizations, they found that the

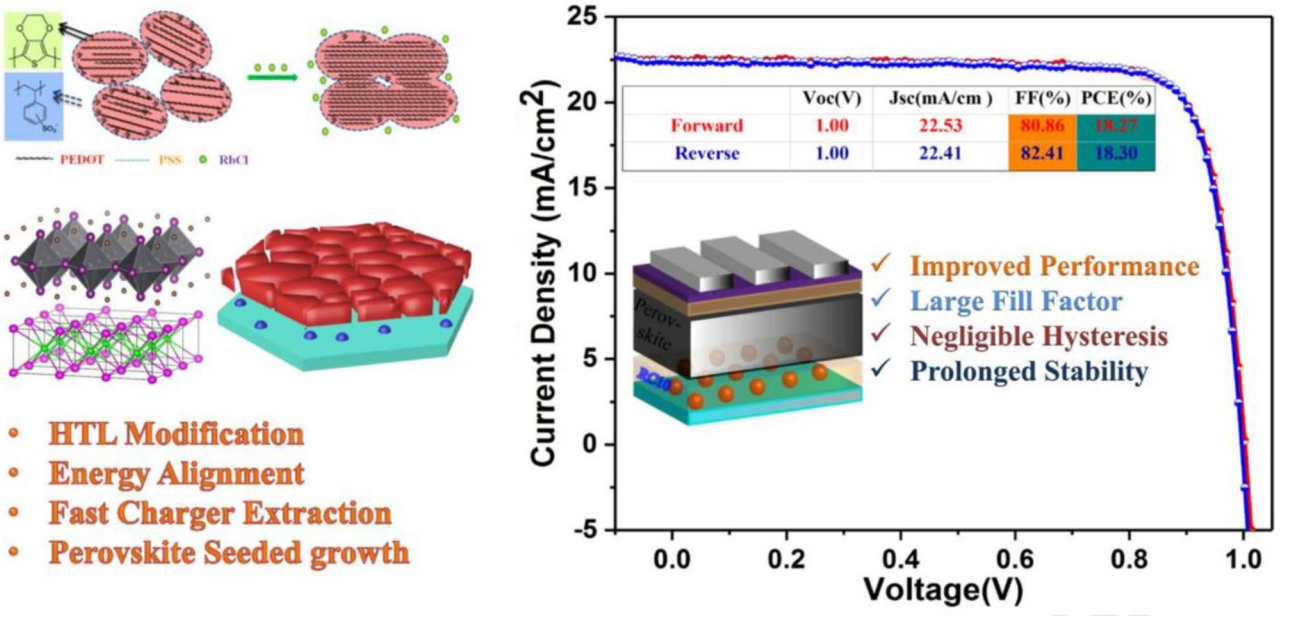

Fig. 3 Schematic model of structural modification and the process of holes' extraction and transport in PEDOT:PSS with the addition of RbCl. *J*−*V* curves of the mixed perovskite based on RbCl-doped PEDOT:PSS [76]

RbCl could induce phase segregation of PEDOT:PSS and enlarge its nanocrystal size, which in turn simultaneously enhance electrical conductivity, hole transport capability and work function without sacrificing optical transmittance of the HTL. The PSCs with the RbCl-doped PEDOT:PSS HTL show remarkably high PCE of 18.3%.

The relatively low work function and high hydrophilicity of PEDOT:PSS hinder the achievement of high power conversion efficiency and device stability. Chang group [71] reported a new water-soluble PEDOT:SAF (sulfonated acetone-formaldehyde) with higher PEDOT content (Fig. 4). PEDOT:SAF showed extremely lower acidity with pH value at around 6 and much higher conductivity of 3.12 S/cm. PEDOT:SAF-based PSC achieved an impressive PCE of 14.05%, which is better than PEDOT:PSS controlled PSC (13.31%). Subsequently, they found a novel and readily available approach to enhancing the work function and waterproofness of PEDOT by copolymerizing dopamine (DA) with a PEDOT backbone [132]. The product, PDA:PEDOT:LS, with a work function of 5.45 eV, matched well with the valence band of the perovskite layer. Moreover, it exhibited much lower acidity, with a pH of 5.3, excellent waterproofness and lowered hydrophilicity.

2.3 Composite and bilayer

For the better HTL fabrication, many trials have been conducted on the use of two different materials to provide synergetic effect on the hole transporting ability. Specifically, the effectiveness of graphene derivatives for composite or bilayer interlayers has been recently reported. Huang et al. [140] and Giuri et al. [141] incorporated reduced graphene

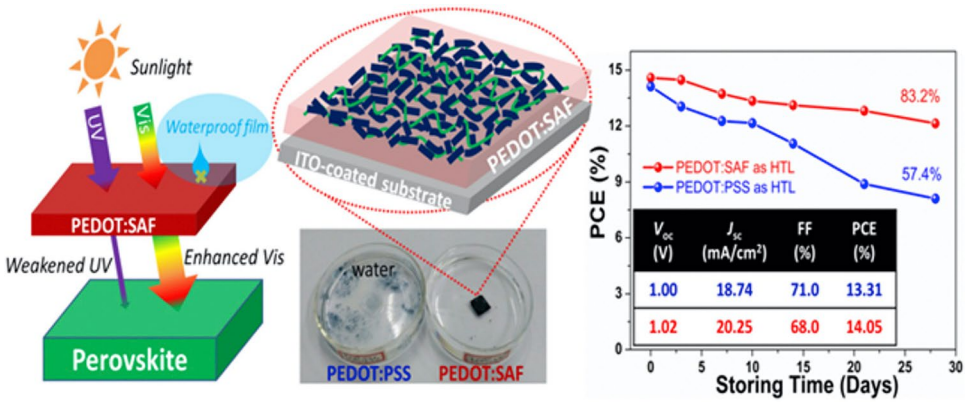

Fig. 4 Chematic diagram for the UV absorbing effect of PEDOT:SAF-based HEL toward pervoskite layer; proposed diagrammatic structures of PEDOT:SAF films on ITO-coated substrate; ptability characteristics of the PSCs using PEDOT:PSS and PEDOT:SAF as the HTLs [71]

oxide (rGO) into PEDOT:PSS. PSCs with rGO/PEDOT:PSS composite as HTL exhibit improved PCE. Mann et al. [116] fabricated PSCs with a bilayer consisting of PEDOT:PSS and sulfonic acid functionalized graphene oxide (SrGO) as a hole interfacial layer. The PEDOT:PSS/SrGO interlayer produced better PCE of 16.01%, which is mostly due to the decreased recombination and the increased built-in potential for better charge transport and extraction. Recently, Li et al. [115] reported PEDOT:PSS/GQDs (Graphene quantum dots) composite film as HTLs of the inverted PSCs, achieving a maximum efficiency of 15.24%.

Some other hole transporting materials, i.e., inorganic metal oxide [117, 130, 135], 2,2′,7,7′-tetrakis(*N*,*N*-di-p-methoxyphenylamine)-9,9′-spirobifluoren (spiro-OMeTAD) [125], and CuSCN [114], have also been employed in PEDOT:PSS for composite or bilayer interlayers as HTL in PSCs. Kegelmann et al. [125] employed mixtures of dopant-free spiro-OMeTAD and water-free PEDOT as an HTL in PSCs. It suggested that surface recombination is suppressed by the PEDOT and charge extraction at the perovskite interface is enhanced by spiro-OMeTAD. This is reflected in the resulting solar cells by increased FFs and highly stabilized efficiencies of up to 18.7%. Recently, Xu et al. [114] fabricated PEDOT:PSS/CuSCN composites as HTLs of the inverted PSCs, achieving a maximum efficiency of 15.3%, which is higher than of the CuSCN-treated PEDOT:PSS-based PSCs [128]. Inorganic metal oxide HTLs, such as Vanadium Pentoxide (V_2O_5), are potentially superior alternatives owning to high carrier mobility with energy levels well suited for hole transport in perovskite solar cells. Wang et al. [135] reported a 15% PSC incorporating V_2O_5 and PEDOT:PSS bilayer as HTL. Other inorganic metal oxide, such as chromium trioxide (CrO_3), has also drawn significant attentions. PEDOT:PSS-CrO_3 composite films can act as a good underlayer for the growth of the crystal perovskite films. Consequently, the resulting PSC device showed a power conversion efficiency (PCE) as high as 16.90% [130]. Recently, Yi et al. [117] reported a 15.1% PSC on tungsten oxide (WO_3) and water-based PEDOT:PSS composite HTL.

3 PEDOT:PSS as a transparent electrode in perovskite solar cells

Most PSCs are built on transparent conductive oxides (TCOs) such as fluorine-doped tin oxide (FTO) or indium tin oxide (ITO), which are costly and rigid. Therefore, it is significant to explore alternative materials as the transparent electrode of PSCs. PEDOT:PSS, owing to its unique physical properties and processability, is a good candidate material as transparent electrode.

In 2015, Ouyang group [79] first reported PEDOT:PSS instead of ITO as the transparent electrode of both rigid and flexible PSCs. The conductivity of PEDOT:PSS films on rigid glass or flexible poly(ethylene terephthalate) (PET) substrate is significantly enhanced through a treatment with methanesulfonic acid (MSA). The optimal PCE is close to 11% for the rigid PSCs with an MSA-treated PEDOT:PSS film as the transparent electrode on glass, and it is more than 8% for the flexible PSCs with an MSA-treated PEDOT:PSS film as the transparent electrode on PET. The flexible PSCs exhibit excellent mechanical flexibility in the bending test (Fig. 5).

In case of conventional PSCs, the top electrode is fabricated by evaporating a metallic electrode onto the active material. The metallic top electrode prevents PSCs from

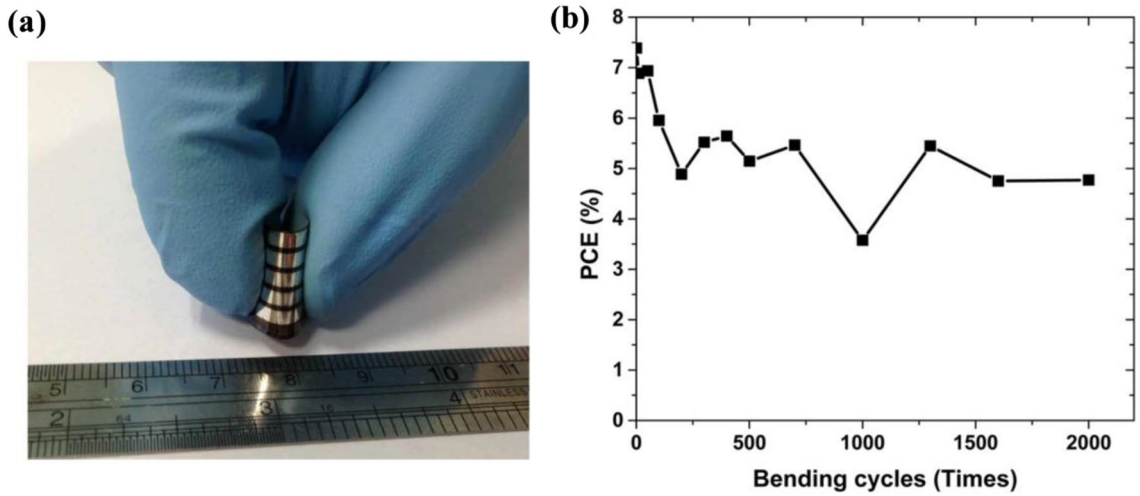

Fig. 5 **a** Photo of a flexible PSC with MSA-PEDOT:PSS/PET. The PSC is deformed manually to a bend radius of 2 mm. **b** Variation of the PCE of a flexible PSC with the bending cycle [79]

being fabricated with solution-based low-temperature, high-volume and large-area processing techniques. Thus, some research groups used PEDOT:PSS as top electrode in PSCs. In 2016, Makha et al. [144] demonstrated a highly transparent laminate electrode for PSCs with stabilized PCE of over 7%. The electrode is composed of a mesh-like silver network on PET, coated with a PEDOT:PSS/sorbitol film. In 2018, Kim et al. [145] fabricated inverted semi-transparent perovskite photovoltaics via stamping transfer at low temperature. Highly conductive and transparent PEDOT:PSS (PH1000) electrode was used as top electrode and the work function was modified through polyethylenimine layer coating on the PH1000 electrode.

4 Conclusions

In conclusion, we summarized the new application of PEDOT:PSS as HTL or electrode in perovskite solar cells. The properties of PEDOT:PSS can be tailored to improve the performance of PSCs by post-treatment, doping, composite and bilayer formation. Furthermore, PEDOT:PSS is demonstrated to be a promising flexible transparent electrode to replace ITO or metallic top electrode of PSCs. Therefore, with its unique opto-electronic properties and excellent processability, to explore the application of PEDOT:PSS in flexible electronics could be an exciting future research direction.

Acknowledgements This research work was supported by the National Science Foundation for Young Scientists of China (61704107), the Young Eastern Scholar (QD2016012) of Shanghai Municipal Education Commission, and the Shanghai Pujiang Program (17PJ1406800).

References

1. R. Po, C. Carbonera, A. Bernardi, F. Tinti, N. Camaioni, Polymer- and carbon-based electrodes for polymer solar cells: toward low-cost, continuous fabrication over large area. Sol. Energy Mater. Sol. Cells **100**, 97–114 (2012)
2. V.R. Feig, H. Tran, M. Lee, Z.N. Bao, Mechanically tunable conductive interpenetrating network hydrogels that mimic the elastic moduli of biological tissue. Nat. Commun. **9**, 2740 (2018)
3. A.K.K. Kyaw, D.H. Wang, V. Gupta, J. Zhang, S. Chand, G.C. Bazan, A.J. Heeger, Efficient solution-processed small-molecule solar cells with inverted structure. Adv. Mater. **25**, 2397 (2013)
4. A. Sharma, G. Andersson, D.A. Lewis, Role of humidity on indium and tin migration in organic photovoltaic devices. Phys. Chem. Chem. Phys. **13**, 4381 (2011)
5. E. Voroshazi, G. Uytterhoeven, K. Cnops, T. Conard, P. Favia, H. Bender, R. Muller, D. Cheyns, Root-cause failure analysis of photocurrent loss in polythiophene: fullerene-based inverted solar cells. ACS Appl. Mater. Interfaces **7**, 618 (2015)
6. V.M. Drakonakis, A. Savva, M. Kokonou, S.A. Choulis, Investigating electrodes degradation in organic photovoltaics through reverse engineering under accelerated humidity lifetime conditions. Sol. Energy Mater. Sol. Cells **130**, 544 (2014)
7. X. Bao, L. Sun, W. Shen, C. Yang, W. Chen, R. Yang, Facile preparation of TiO_X film as an interface material for efficient inverted polymer solar cells. J. Mater. Chem. A **2**, 1732 (2014)
8. X. Fan, C. Cui, G. Fang, J. Wang, S. Li, F. Cheng, H. Long, Y. Li, Efficient polymer solar cells based on poly(3-hexylthiophene):indene-C_{70} bisadduct with a MoO_3 buffer layer. Adv. Funct. Mater. **22**, 585 (2012)
9. S.I. Na, S.S. Kim, J. Jo, D.Y. Kim, Efficient and flexible ITO-free organic solar cells using highly conductive polymer anodes. Adv. Mater. **20**, 4061 (2008)
10. F. Ely, A. Matsumoto, B. Zoetebier, V. Peressinotto, M. Hirata, D. Sousa, R. Maciel, Handheld and automated ultrasonic spray deposition of conductive PEDOT:PSS films and their application in AC EL devices. Org. Electron. **15**, 1062 (2014)
11. S. Allard, M. Forster, B. Souharce, H. Thiem, U. Scherf, Organic semiconductors for solution-processable field-effect transistors (OFETs). Angew. Chem., Int. Ed. **47**, 4070 (2008)
12. Y. Xia, K. Sun, J. Ouyang, Solution-processed metallic conducting polymer films as transparent electrode of optoelectronic devices. Adv. Mater. **24**, 2436 (2012)
13. N. Kim, S. Kee, S.H. Lee, B.H. Lee, Y.H. Kahng, Y.-R. Jo, B.-J. Kim, K. Lee, Highly conductive PEDOT: PSS nanofibrils induced by solution-processed crystallization. Adv. Mater. **26**, 2268 (2014)
14. N. Kim, H. Kang, J.-H. Lee, S. Kee, S.H. Lee, K. Lee, Highly conductive all-plastic electrodes fabricated using a novel chemically controlled transfer-printing method. Adv. Mater. **27**, 2317 (2015)
15. X. Fan, B. Xu, S. Liu, C. Cui, J. Wang, F. Yan, Transfer-printed PEDOT: PSS electrodes using mild acids for high conductivity and improved stability with application to flexible organic solar cells. ACS Appl. Mater. Interfaces **8**, 14029 (2016)
16. J.Y. Kim, J.H. Jung, D.E. Lee, J. Joo, Enhancement of electrical conductivity of poly (3,4-ethylenedioxythiophene)/poly (4-styrenesulfonate) by a change of solvents. Synth. Met. **126**, 311–316 (2002)
17. J. Ouyang, Q. Xu, C. Chu, Y. Yang, G. Li, J. Shinar, On the mechanism of conductivity enhancement in poly (3,4-ethylen edioxythiophene):poly (styrenesulfonate) film through solvent treatment. Polymer **45**, 8443–8450 (2004)
18. X. Crispin, F.L.E. Jakobsson, A. Crispin, P.C.M. Grim, P. Andersson, A. Volodin, C. Van Haesendonck, M.Va.n der Auweraer, W.R. Salaneck, M.Berggren, The origin of the high conductivity of poly (3,4-ethylenedioxythiophene)–poly (styrenesulfonate)(PEDOT-PSS) plastic electrodes. Chem. Mater. **18**, 4354–4360 (2006)
19. A.M. Nardes, R.A.J. Janssen, M.A. Kemerink, A morphological model for the solvent-enhanced conductivity of PEDOT: PSS thin films. Adv. Funct. Mater. **18**, 865–871 (2008)
20. M. Döbbelin, R. Marcilla, M. Salsamendi, C. Pozo-Gonzalo, P.M. Carrasco, J.A. Pompos, D. Mecerreyes, Influence of ionic liquids on the electrical conductivity and morphology of PEDOT:PSS films. Chem. Mater. **19**, 2147–2149 (2007)
21. B.H. Fan, X.G. Mei, J. Ouyang, Significant conductivity enhancement of conductive poly(3,4-ethylenedioxythiophene):poly- (styrenesulfonate) films by adding anionic surfactants into polymer solution. Macromolecules **41**, 5971–5973 (2008)
22. L.A.A. Pettersson, S. Ghosh, O. Inganäs, Optical anisotropy in thin films of poly(3,4-ethylenedioxythiophene)–poly(4-styrenesulfonate). Org. Electron. **3**, 143–148 (2002)
23. S.K.M. Jönsson, J. Birgerson, X. Crispin, G. Greczynski, W. Osikowicz, A.W.D.V.D. Gon, W.R. Salaneck, M. Fahlman, The effects of solvents on the morphology and sheet resistance in poly (3, 4-ethylenedioxythiophene)- polystyrenesulfonic acid (PEDOT-PSS) films. Synth. Met. **139**, 1–10 (2003)

24. M. Reyes-Reyes, I. Cruz-Cruz, R. Lopez-Sandoval, Enhancement of the electrical conductivity in PEDOT:PSS films by the addition of dimethyl Sulfate. J. Phys. Chem. C **114**, 20220–20224 (2010)
25. Y. Xia, J. Ouyang, Salt-induced charge screening and significant conductivity enhancement of conducting poly (3, 4-ethylenedioxythiophene): poly (styrenesulfonate). Macromolecules **42**, 4141–4147 (2009)
26. Y. Xia, H.M. Zhang, J. Ouyang, Highly conductive PEDOT: PSS films prepared through a treatment with zwitterions and their application in polymer photovoltaic cells. J. Mater. Chem. **20**, 9740–9747 (2010)
27. Y. Xia, J. Ouyang, PEDOT:PSS films with significantly enhanced conductivities induced by preferential solvation with cosolvents and their application in polymer photovoltaic cells. J. Mater. Chem. **21**, 4927–4936 (2011)
28. Y. Xia, J. Ouyang, Anion effect on salt-induced conductivity enhancement of poly (3, 4-ethylenedioxythiophene): poly (styrenesulfonate) films. Anion effect on salt-induced conductivity enhancement of poly (3, 4-ethylenedioxythiophene): poly (styrenesulfonate) films. Org. Electron. **11**, 1129–1135 (2010)
29. Y.H. Kim, C. Sachse, M.L. Machala, C. May, L. Müller-Meskamp, K. Leo, Highly conductive PEDOT:PSS electrode with optimized solvent and thermal post-treatment for ITO-free organic solar cells. Adv. Funct. Mater. **21**, 1076–1081 (2011)
30. Y. Xia, K. Sun, J. Ouyang, Highly conductive poly (3,4-ethyl enedioxythiophene):poly (styrenesulfonate) films treated with an amphiphilic fluoro compound as the transparent electrode of polymer solar cells. Energy Environ. Sci. **5**, 5325–5332 (2012)
31. Y. Xia, K. Sun, J. Chang, J. Ouyang, Effects of organic inorganic hybrid perovskite materials on the electronic properties and morphology of poly (3, 4-ethylenedioxythiophene): poly(styrenesulfonate) and the photovoltaic performance of planar perovskite solar cells. J. Mater. Chem. A **3**, 15897–15904 (2015)
32. D.J. Lipomi, M. Vosgueritchian, B.C. Tee, S.L. Hellstrom, J.A. Lee, C.H. Fox, Z. Bao, Skin-like pressure and strain sensors based on transparent elastic films of carbon nanotubes. Nat. Nanotechnol. **6**, 788 (2011)
33. C.Z. Liao, M. Zhang, L.Y. Niu, Z.J. Zheng, F. Yan, Highly selective and sensitive glucose sensors based on organic electrochemical transistors with graphene-modified gate electrodes. J. Mater. Chem. B **1**, 3820 (2013)
34. C.Z. Liao, C.H. Mak, M. Zhang, H.L.W. Chan, F. Yan, Flexible organic electrochemical transistors for highly selective enzyme biosensors and used for saliva testing. Adv. Mater. **27**, 676 (2015)
35. I. Agua, D. Mantione, U. Ismailov, A. Sanchez-Sanchez, N. Aramburu, G.G. Malliaras, D. Mecerreyes, E. Ismailova, DVS-crosslinked PEDOT:PSS free-standing and textile electrodes toward wearable health monitoring. Adv. Mater. Technol. **3**, 1700322 (2018)
36. X. Fan, B. Xu, N.X. Wang, J.Z. Wang, S.H. Liu, H. Wang, F. Yan, Highly conductive stretchable all-plastic electrodes using a novel dipping-embedded transfer method for high-performance wearable sensors and semitransparent organic solar cells. Adv. Electron. Mater. **3**, 1600471 (2017)
37. S.C.B. Mannsfeld, B.C.K. Tee, R.M. Stoltenberg, C.V.H.H. Chen, S. Barman, B.V.O. Muir, A.N. Sokolov, C. Reese, Z. Bao, Highly sensitive flexible pressure sensors with microstructured rubber dielectric layers. Nat. Mater. **9**, 859 (2010)
38. D.J. Cohen, D. Mitra, K. Peterson, M.M. Maharbiz, A highly elastic, capacitive strain gauge based on percolating nanotube networks. Nano Lett. **12**, 1821 (2012)
39. J.-Y. Sun, C. Keplinger, G.M. Whitesides, Z. Suo, Ionic skin. Adv. Mater. **26**, 7608 (2014)
40. J. Jeon, H. Lee, Z. Bao, Flexible wireless temperature sensors based on Ni microparticle-filled binary polymer composites. Adv. Mater. **25**, 850 (2013)
41. H. Yang, D. Qi, Z. Liu, B.K. Chandran, T. Wang, J. Yu, X. Chen, Soft thermal sensor with mechanical adaptability. Adv. Mater. **28**, 9175 (2016)
42. S. Gong, W.L. Cheng, One-dimensional nanomaterials for soft electronics. Adv. Electron. Mater. **3**, 1600314 (2017)
43. S. Gong, D.T.H. Lai, B. Su, K.J. Si, Z. Ma, L.W. Yap, P.Z. Guo, W.L. Cheng, Highly stretchy black gold e-skin nanopatches as highly sensitive wearable biomedical sensors. Adv. Electron. Mater. **1**, 1400063 (2015)
44. A. Chortos, J. Liu, Z. Bao, Pursuing prosthetic electronic skin. Nat. Mater. **15**, 937 (2016)
45. R.C. Webb, A.P. Bonifas, A. Behnaz, Y. Zhang, K.J. Yu, H. Cheng, M. Shi, Z. Bian, Z. Liu, Y.-S. Kim, W.-H. Yeo, J.S. Park, J. Song, Y. Li, Y. Huang, A.M. Gorbach, J.A. Rogers, Ultrathin conformal devices for precise and continuous thermal characterization of human skin. Nat. Mater. **12**, 938 (2013)
46. Y.-C. Lai, J. Deng, S. Niu, W. Peng, C. Wu, R. Liu, Z. Wen, Z.L. Wang, Electric eel-skin-inspired mechanically durable and super-stretchable nanogenerator for deformable power source and fully autonomous conformable electronic-skin applications. Adv. Mater. **28**, 10024 (2016)
47. Y. Xia, J. Fang, P. Li, B. Zhang, H. Yao, J. Chen, J. Ding, J. Ouyang, Solution-processed highly superparamagnetic and conductive PEDOT:PSS/Fe3O4 nanocomposite films with high transparency and high mechanical flexibility. ACS Appl. Mater. Interfaces **9**, 19001–19010 (2017)
48. J. Ouyang, 'Secondary doping' methods to significantly enhance the conductivity of PEDOT:PSS for its application as transparent electrode of optoelectronic devices. Displays **34**, 423–436 (2013)
49. H. Shi, C. Liu, Q. Jiang, J. Xu, Effective approaches to improve the electrical conductivity of PEDOT:PSS: a review. Adv. Electron. Mater. **1**, 1500017 (2015)
50. K. Sun, S. Zhang, P. Li, Y. Xia, X. Zhang, D. Du, F. Isikgor, J. Ouyang, Review on application of PEDOTs and PEDOT:PSS in energy conversion and storage devices. J. Mater. Sci.: Mater. Electron. **26**, 4438–4462 (2015)
51. H. Yao, Z. Fan, H. Cheng, X. Guan, C. Wang, K. Sun, J. Ouyang, Recent development of thermoelectric polymers and composites. Macromol. Rapid Commun. **39**, 1700727 (2018)
52. X. Fan, W. Nie, H. Tsai, N. Wang, H. Huang, Y. Cheng, R. Wen, M. Liujia, F. Yan, Y. Xia, PEDOT:PSS for flexible and stretchable electronics: modifications, strategies, and applications. Adv. Sci. **6**, 1900813 (2019)
53. Q. Qiao, *Organic Solar Cells*, 1st edn. (CRC Press, Boca Raton, 2017), p. 44
54. Z. C.Yang, Y. Sun, B. He, S. Xiong, M. Chen, Y. Li, Y. Zhou, K. Zheng, Sun, Performance-enhancing approaches for the pedot:pss-si hybrid solar cells. Angew. Chem. Int. Ed. (2019). https://doi.org/10.1002/anie.201910629
55. H.-S. Kim, C.-R. Lee, J.-H. Im, K.-B. Lee, T. Moehl, A. Marchioro, S.-J. Moon, R. Humphry-Baker, J.-H. Yum, J.E. Moser, M. Grätzel, N.-G. Park, Lead iodide perovskite sensitized all-solid-state submicron thin film mesoscopic solar cell with efficiency exceeding 9%. Sci. Rep. **2**, 591 (2012)
56. M.D. McGehee, Perovskite solar cells: continuing to soar. Nat. Mater. **13**, 845–846 (2014)
57. M. Grätzel, The light and shade of perovskite solar cells. Nat. Mater. **13**, 838–842 (2014)
58. M.C. Beard, J.M. Luther, A.J. Nozik, The promise and challenge of nanostructured solar cells. Nat. Nanotechnol. **9**, 951–954 (2014)

59. J. Jean, P.R. Brown, R.L. Jaffe, T. Buonassisi, V. Bulović, Pathways for solar photovoltaics. Energy Environ. Sci. **8**, 1200–1219 (2015)
60. K. Wang, C. Liu, P. Du, J. Zheng, X. Gong, Bulk heterojunction perovskite hybrid solar cells with large fill factor. Energy Environ. Sci. **8**, 1245–1255 (2015)
61. B.J. Kim, D.H. Kim, Y.Y. Lee, H.W. Shin, G.S. Han, J.S. Hong, K. Mahmood, T.K. Ahn, Y.C. Joo, K.S. Hong, N.G. Park, S. Lee, H.S. Jung, Highly efficient and bending durable perovskite solar cells: toward a wearable power source. Energy Environ. Sci. **8**, 916–921 (2015)
62. C.D. Bailie, M.G. Christoforo, J.P. Mailoa, A.R. Bowring, E.L. Unger, W.H. Nguyen, J. burschka, N. Pellet, J.Z. Lee, M. Grätzel, R. Noufi, T. Buonassisi, A. Salleo, M.D. McGehee, Semi-transparent perovskite solar cells for tandems with silicon and CIGS. Energy Environ. Sci. **8**, 956–963 (2015)
63. D. Liu, T.L. Kelly, Perovskite solar cells with a planar heterojunction structure prepared using room-temperature solution processing techniques. Nat. Photonics **8**, 133–138 (2014)
64. D. Bryant, P. Greenwood, J. Troughton, M. Wijdekop, M. Carnie, M. Davies, K. Wojciechowski, H.J. Snaith, T. Watson, D. Worsley, A transparent conductive adhesive laminate electrode for high-efficiency organic-inorganic lead halide perovskite solar cells. Adv. Mater. **26**, 7499–7504 (2014)
65. N.K. Noel, A. Abate, S.D. Stranks, E.S. Parrott, V.M. Burlakov, A. Goriely, H.J. Snaith, Enhanced photoluminescence and solar cell performance via lewis base passivation of organic–inorganic lead halide perovskites. ACS Nano **8**, 9815–9821 (2014)
66. J.S. Manser, P.V. Kamat, Band filling with free charge carriers in organometal halide perovskites. Nat. Photonics **8**, 737–743 (2014)
67. J. Chang, H. Zhu, B. Li, F. Isikgor, Y. Hao, Q. Xu, J. Ouyang, Boosting the performance of planar heterojunction perovskite solar cell by controlling the precursor purity of perovskite materials. J. Mater. Chem. A **4**, 887–893 (2016)
68. J. Chang, H. Zhu, J. Xiao, F. Isikgor, Z. Lin, Y. Hao, K. Zeng, Q. Xu, J. Ouyang, Enhancing the planar heterojunction perovskite solar cells performance through tuning precursor ratio. J. Mater. Chem. A **4**, 7943–7949 (2016)
69. J. Chang, Z. Lin, H. Zhu, F. Isikgor, Q. Xu, C. Zhang, Y. Hao, J. Ouyang, Enhancing the photovoltaic performance of planar heterojunction perovskite solar cells by doping the perovskite layer with alkali metal ions. J. Mater. Chem. A **4**, 16546–16552 (2016)
70. L. Zhou, J. Chang, Z. Liu, X. Sun, Z. Lin, D. Chen, C. Zhang, J. Zhang, Y. Hao, Enhanced planar perovskite solar cell efficiency and stability using a perovskite/PCBM heterojunction formed in one-step. Nanoscale **10**, 3053–3059 (2018)
71. W. Yu, K. Wang, B. Guo, X. Qiu, Y. Hao, J. Chang, Y. Li, Effect of ultraviolet absorptivity and waterproofness of poly (3, 4-ethylenedioxythiophene) with extremely weak acidity, high conductivity on enhanced stability of perovskite solar cells. J. Power Sources **358**, 29–38 (2017)
72. J. Huang, C. Wang, Z. Liu, X. Qiu, J. Yang, J. Chang, Simultaneously enhanced durability and performance by employing dopamine copolymerized PEDOT with high work function and water-proofness for inverted perovskite solar cells. J. Mater. Chem. C **6**, 2311–2318 (2018)
73. Z. Lin, J. Chang, J. Xiao, H. Zhu, Q. Xu, C. Zhang, J. Ouyang, Y. Hao, Interface studies of the planar heterojunction perovskite solar cells. Sol. Energy Mater. Sol. Cells **157**, 783–790 (2016)
74. Z. Lin, J. Zhou, L. Zhou, K. Wang, W. Li, J. Su, Y. Hao, Y. Li, J. Chang, Simultaneously enhanced performance and stability of inverted perovskite solar cells via a rational design of hole transport layer. Org. Electron. **73**, 69–75 (2019)
75. L. Hu, J. Fu, K. Yang, Z. Xiong, M. Wang, B. Yang, X. Wang, X. Tang, Z. Zang, Inhibition of in-plane charge transport in hole transfer layer to achieve high fill factor for inverted planar perovskite solar cells. Solar RRL **3**, 1900104 (2019)
76. X. Liu, B. Li, N. Zhang, Z. Yu, K. Sun, B. Tang, D. Shi, H. Yao, J. Ouyang, Multifunctional RbCl dopants for efficient inverted planar perovskite solar cell with ultra-high fill factor, negligible hysteresis and improved stability. Nano Energy **53**, 567–578 (2018)
77. L. Hu, M. Li, K. Yang, Z. Xiong, B. Yang, M. Wang, X. Tang, Z. Zang, X. Liu, B. Li, Z. Xiao, S. Lu, H. Gong, J. Ouyang, K. Sun, PEDOT:PSS monolayers to enhance hole extraction and stability of perovskite solar cells. J. Mater. Chem. A **6**, 16583–16589 (2018)
78. L. Hu, K. Sun, M. Wang, W. Chen, B. Yang, J. Fu, Z. Xiong, X. Li, X. Tang, Z. Zang, S. Zhang, L. Sun, M. Li, Inverted planar perovskite solar cells with a high fill factor and negligible hysteresis by the dual effect of NaCl-doped PEDOT: PSS. ACS Appl. Mater. Interfaces **9**, 50, 43902–43909 (2017)
79. K. Sun, P. Li, Y. Xia, J. Chang, J. Ouyang, Transparent conductive oxide-free perovskite solar cells with PEDOT: PSS as transparent electrode. ACS Appl. Mater. Interfaces **7**(28), 15314–15320 (2015)
80. S. Zhang, Z. Yu, P. Li, B. Li, F.H. Isikgor, D. Du, K. Sun, Y. Xia, J. Ouyang, Poly(3,4-ethylenedioxythiophene):polystyrene sulfonate films with low conductivity and low acidity through a treatment of their solutions with probe ultrasonication and their application as hole transport layer in polymer solar cells and perovskite solar cells. Org. Electron. **32**, 149–156 (2016)
81. K. Sun, J. Chang, F.H. Isikgor, P. Li, J. Ouyang, Efficiency enhancement of planar perovskite solar cells by adding zwitterion/LiF double interlayers for electron collection. Nanoscale **7**(3), 896–900 (2015)
82. Best research-cell efficiency chart, NREL (2019). https://www.nrel.gov/pv/cell-efficiency.html.
83. S.D. Stranks, G.E. Eperon, G. Grancini, C. Menelaou, M.J.P. Alcocer, T. Leijtens, L.M. Herz, A. Petrozza, H.J. Snaith, Electron-hole diffusion lengths exceeding 1 micrometer in an organometal trihalide perovskite absorber. Science **342**, 341–344 (2013)
84. C.H. Wang, C.J. Zhang, S.T. Wang, G. Liu, H.Y. Xia, S.C. Tong, J. He, D.M. Niu, C.H. Zhou, K.X. Ding, Y.L. Gao, J.L. Yang, Low-temperature processed, efficient, and highly reproducible cesium-doped triple cation perovskite planar heterojunction solar cells. Sol. RRL **2**, 1700209 (2018)
85. W.J. Yin, T.T. Shi, Y.F. Yan, Unusual defect physics in $CH_3NH_3PbI_3$ perovskite solar cell absorber. Appl. Phys. Lett. **104**, 063903 (2014)
86. C. Wehrenfennig, G.E. Eperon, M.B. Johnston, H.J. Snaith, L.M. Herz, High charge carrier mobilities and lifetimes in organolead trihalide perovskites. Adv. Mater. **26**, 1584–1589 (2014)
87. Q. Dong, Y. Fang, Y. Shao, P. Mulligan, J. Qiu, L. Cao, J. Huang, Electron-hole diffusion lengths > 175 μm in solution-grown $CH_3NH_3PbI_3$ single crystals. Science **347**, 967–970 (2015)
88. G. Xing, N. Mathews, S. Sun, S.S. Lim, Y.M. Lam, M. Gřatzel, S. Mhaisalkar, T.C. Sum, Long-range balanced electron- and hole-transport lengths in organic-inorganic$CH_3NH_3PbI_3$. Science **342**, 344–347 (2013)
89. K.O. Brinkmann, J. Zhao, N. Pourdavoud, T. Becker, T. Hu, S. Olthof, K. Meerholz, L. Hoffmann, T. Gahlmann, R. Heiderhoff, M.F. Oszajca, N.A. Luechinger, D. Rogalla, Y. Chen, B. Cheng, T. Riedl, Suppressed decomposition of organometal halide perovskites by impermeable electron-extraction layers in inverted solar cells. Nat. Commun. **8**, 13938 (2017)
90. Z.G. Xiao, C. Bi, Y.C. Shao, Q.F. Dong, Q. Wang, Y.B. Yuan, C.G. Wang, Y.L. Gao, J.S. Huang, Efficient, high yield perovskite photovoltaic devices grown by interdiffusion of

solution-processed precursor stacking layers. Energy Environ. Sci. **7**, 2619–2623 (2014)
91. P.W. Liang, C.Y. Liao, C.C. Chueh, F. Zuo, S.T. Williams, X.K. Xin, J.J. Lin, A.K.Y. Jen, Additive enhanced crystallization of solution-processed perovskite for highly efficient planar-heterojunction solar cells. Adv. Mater. **26**, 3748–3754 (2014)
92. H. Azimi, T. Ameri, H. Zhang, Y. Hou, C.O.R. Quiroz, J. Min, M.Y. Hu, Z.G. Zhang, T. Przybilla, G.J. Matt, E. Spiecker, Y.F. Li, C.J. Brabec, A universal interface layer based on an amine-functionalized fullerene derivative with dual functionality for efficient solution processed organic and perovskite solar cells. Adv. Energy Mater. **5**, 1401692 (2015)
93. C. Sun, Z.H. Wu, H.L. Yip, H. Zhang, X.F. Jiang, Q.F. Xue, Z.C. Hu, Z.H. Hu, Y. Shen, M.K. Wang, F. Huang, Y. Cao, Amino-functionalized conjugated polymer as an efficient electron transport layer for high-performance planar-heterojunction perov- skite solar cells. Adv. Energy Mater. **6**, 1501534 (2016)
94. Y. Yao, G. Wang, L. Liao, D. Liu, G. Zhou, C. Xu, X. Yang, R. Wu, Q. Song, Enhancing the open circuit voltage of PEDOT:PSS-PC_{61}BM based inverted planar mixed halide perovskite solar cells from 0.93 to 1.05 V by simply oxidizing PC_{61} BM. Org. Electron. **59**, 260–265 (2018)
95. X.Y. Zhou, Y. Zhang, W.G. Kong, M.M. Hu, L.Z. Zhang, C. Liu, X.N. Li, C.Y. Pan, G.P. Yu, C. Cheng, B.M. Xu, Crystallization manipulation and morphology evolution for highly efficient perovskite solar cell fabrication via hydration water induced intermediate phase formation under heat assisted spin-coating. J. Mater. Chem. **6**, 3012 (2018)
96. W.S. Yang, B.W. Park, E.H. Jung, N.J. Jeon, Y.C. Kim, D.U. Lee, S.S. Shin, J.G. Seo, E.K. Kim, J.H. Noh, S.I. Seok, Iodide management in formamidinium–lead–halide-based perovskite layers for efficient solar cells. Science **356**, 1376 (2017)
97. Q. Wang, Y. Shao, Q. Dong, Z. Xiao, Y. Yuan, J.S. Huang, Large fill-factor bilayer iodine perovskite solar cells fabricated by a low-temperature solution-process. Energy Environ. Sci. **7**, 2359 (2014)
98. K. Wang, C. Liu, P. Du, J. Zheng, X. Gong, Bulk heterojunction perovskite hybrid solar cells with large fill factor. Energy Environ. Sci. **8**, 1245 (2015)
99. J.W. Lee, H.S. Kim, N.G. Park, Lewis acid–base adduct approach for high efficiency perovskite solar cells. Acc. Chem. Res. **49**, 311 (2016)
100. C. Liu, K. Wang, P. Du, C. Yi, T. Meng, X. Gong, Efficient solution-processed bulk heterojunction perovskite hybrid solar cells. Adv. Energy Mater. **5**, 1402024 (2015)
101. C.H. Chiang, Z.L. Tseng, C.G. Wu, Planar heterojunction perovskite/PC71BM solar cells with enhanced open-circuit voltage via a (2/1)-step spin-coating process. J. Mater. Chem. A **2**, 15897 (2014)
102. M. Wolf, H. Rauschenbach, Series resistance effects on solar cell measurements. Adv. Energy Convers. **3**, 455 (1963)
103. C. Yi, A. Wilhite, L. Zhang, R. Hu, S.S. Chuang, J. Zheng, X. Gong, Enhanced thermoelectric properties of poly(3,4-ethylen edioxythiophene):poly(styrenesulfonate) by binary secondary dopants. ACS Appl. Mater. Interfaces **7**, 8984 (2015)
104. D. Pysch, A. Mette, S.W. Glunz, A review and comparison of different methods to determine the series resistance of solar cells. Sol. Energy Mater. Sol. Cells **91**, 1698 (2007)
105. X. Huang, K. Wang, C. Yi, T. Meng, X. Gong, Efficient perovskite hybrid solar cells by highly electrical conductive PEDOT: PSS hole transport layer. Adv. Energy Mater. **6**, 1501773 (2016)
106. D.Y. Liu, Y. Li, J.Y. Yuan, Q.M. Hong, G.Z. Shi, D. Yuan, J. Wei, C.C. Huang, J. Tang, M.K. Fung, Improved performance of inverted planar perovskite solar cells with F4-TCNQ doped PEDOT:PSS hole transport layers. J. Mater. Chem. **5**, 5701 (2017)
107. J. Ouyang, C.W. Chu, F.C. Chen, Q. Xu, Y. Yang, High-conductivity poly(3,4-ethylenedioxythiophene):poly(styrene sulfonate) film and Its application in polymer optoelectronic devices. Adv. Funct. Mater. **15**, 203 (2005)
108. F.J. Lim, K. Ananthanarayanan, J. Luther, G.W. Ho, Influence of a novel fluorosurfactant modified PEDOT:PSS hole transport layer on the performance of inverted organic solar cells. J. Mater. Chem. **22**, 25057 (2012)
109. V.D. Mihailetchi, J.K.V. Duren, P.W. Blom, J.C. Hummelen, R.A. Janssen, J.M. Kroon, M.T. Rispens, W.H. Verhees, M.M. Wienk, Electron transport in a methanofullerene. Adv. Funct. Mater. **13**, 43 (2003)
110. D.-Y. Lee, S.-I. Na, S.-S. Kim, Graphene oxide/PEDOT:PSS composite hole transport layer for efficient and stable planar heterojunction perovskite solar cells. Nanoscale **8**, 1513 (2016)
111. A. Giuri, S. Masi, S. Colella, A. Kovtun, S. Dell'Elce, E. Treossi, A. Liscio, C.E. Corcione, A. Rizzo, A. Listorti, Cooperative effect of go and glucose on pedot:pss for high voc and hysteresis-free solution-processed perovskite solar cells. Adv. Funct. Mater. **26**, 6985 (2016)
112. D. Huang, T. Goh, J. Kong, Y. Zheng, S. Zhao, Z. Xu, A. Taylor, Perovskite solar cells with a DMSO-treated PEDOT:PSS hole transport layer exhibit higher photovoltaic performance and enhanced durability. Nanoscale **9**, 4236 (2017)
113. L. Hu, K. Sun, M. Wang, W. Chen, B. Yang, J. Fu, Z. Xiong, X. Li, Z. Zang, S. Zhang, L. Sun, M. Li, Inverted planar perovskite solar cells with a high fill factor and negligible hysteresis by the dual effect of NaCl-doped PEDOT:PSS. ACS Appl. Mater. Interfaces **9**, 43902 (2017)
114. L. Xu, Y. Li, C. Zhang, Y. Liu, C. Zheng, W. Lv, M. Li, Y. Chen, W. Huang, R. Chen, Improving the efficiency and stability of inverted perovskite solar cells by CuSCN-doped PEDOT:PSS. Sol. Energy Mater. Sol. Cells **206**, 110316 (2020)
115. W. Li, N. Cheng, Y. Cao, Z. Zhao, Z. Xiao, W. Zi, Z. Sun, Boost the performance of inverted perovskite solar cells with PEDOT:PSS/graphene quantum dots composite hole transporting layer. Org. Electron. **78**, 105575 (2019)
116. D.S. Mann, Y.-H. Seo, S.-N. Kwon, S.-I. Na, Efficient and stable planar perovskite solar cells with a PEDOT:PSS/SrGO hole interfacial layer. J. Alloys Compd. **812**, 152091 (2020)
117. H. Yi, D. Wang, L. Duan, F. Haque, C. Xu, Y. Zhang, G. Conibeer, A. Uddin, Solution-processed WO_3 and water-free PEDOT:PSS composite for hole transport layer in conventional perovskite solar cell. Electrochim. Acta **319**, 349 (2019)
118. X. Zhou, M. Hu, C. Liu, L. Zhang, X. Zhong, X. Li, Y. Tian, C. Cheng, B. Xu, Synergistic effects of multiple functional ionic liquid-treated PEDOT:PSS and less-ion-defects S-acetylthiocholine chloride-passivated perovskite surface enabling stable and hysteresis-free inverted perovskite solar cells with conversion efficiency over 20%. Nano Energy **63**, 103866 (2019)
119. Y. Zhu, S. Wang, R. Ma, C. Wang, The improvement of inverted perovskite solar cells by the introduction of CTAB into PEDOT:PSS. Sol. Energy **188**, 28 (2019)
120. Y. Wang, Y. Hu, D. Han, Q. Yuan, T. Cao, N. Chen, D. Zhou, H. Cong, L. Feng, Ammonia-treated graphene oxide and PEDOT:PSS as hole transport layer for high-performance perovskite solar cells with enhanced stability. Org. Electron. **70**, 63 (2019)
121. W. Hu, C.Y. Xu, L. Niu, E.A. Mourtada, G. Wang, D. Liu, Y.Q. Yao, L.P. Liao, G.D. Zhou, Q. Song, High open circuit voltage of 1.134 V for inverted planar perovskite solar cells with sodium citrate doped PEDOT:PSS as a hole transport layer. ACS Appl. Mater. Interfaces **11**, 22021 (2019)
122. R. Zhang, H. Ling, X. Lu, J. Xia, The facile modification of PEDOT:PSS buffer layer by polyethyleneglycol and their effects on inverted perovskite solar cell. Sol. Energy **186**, 398 (2019)

123. L. Hu, J. Fu, K. Yang, Z. Xiong, M. Wang, B. Yang, H. Wang, X. Tang, Z. Zang, M. Li, J. Li, K. Sun, Inhibition of in-plane charge transport in hole transfer layer to achieve high fill factor for inverted planar perovskite solar cells. Solar. RRL **3**, 1900104 (2019)
124. D. Shin, D. Kang, J.-B. Lee, J.-H. Ahn, I.-W. Cho, M.-Y. Ryu, S.W. Cho, N.E. Jung, H. Lee, Y. Yi, Electronic structure of non-ionic surfactant-modified PEDOT:PSS and its application in perovskite solar cells with reduced interface recombination. ACS Appl. Mater. Interfaces **11**, 17028 (2019)
125. L. Kegelmann, P. Tockhorn, C.M. Wolff, J.A. Márquez, S. Caicedo-Dávila, L. Korte, T. Unold, W. Lövenich, D. Neher, B. Rech, S. Albrecht, Mixtures of dopant-free Spiro-OMeTAD and water-free PEDOT as passivating hole contact in perovskite solar cells. ACS Appl. Mater. Interfaces **11**, 9172 (2019)
126. P. Fan, D. Zheng, Y. Zheng, J. Yu, Efficient and stable planar p-i-n perovskite solar cells by doping tungsten compound into PEDOT:PSS to facilitate perovskite crystalline. Electrochim. Acta **283**, 922 (2018)
127. H. Li, C. Zhang, Y. Ma, Y. Mai, Y. Xu, Alanine induced structure reconstruction of PEDOT:PSS films in perovskite solar cells. Org. Electron. **62**, 468 (2018)
128. Q. Xiong, H. Tian, J. Zhang, L. Han, C. Lu, B. Shen, Y. Zhang, Y. Zheng, C. Lu, Z. Zeng, Z. Hu, L. Wu, Y. Zhu, CuSCN modified PEDOT:PSS to improve the efficiency of low temperature processed perovskite solar cells. Org. Electron. **61**, 151 (2018)
129. B.J. Bruijnaers, E. Schiepers, C.H.L. Weijtens, S.C.J. Meskers, M.M. Wienk, R.A.J. Janssen, The effect of oxygen on the efficiency of planar p-i-n metal halide perovskite solar cells with a PEDOT:PSS hole transport layer. J. Mater. Chem. A **6**, 6882 (2018)
130. J.-Y. Zhu, K. Niu, M. Li, M.-Q. Lin, J.-H. Li, Z.-K. Wang, PEDOT:PSS-CrO_3 composite hole-transporting layer for high-performance p-i-n structure perovskite solar cells. Org. Electron. **54**, 9 (2018)
131. Z. Sun, Y. Xiahou, T. Cao, K. Zhang, Z. Wang, P. Huang, K. Zhu, L. Yuan, Y. Zhou, B. Song, H. Xia, N. Chen, Enhanced p-i-n type perovskite solar cells by doping AuAg@AuAg core-shell alloy nanocrystals into PEDOT:PSS layer. Org. Electron. **52**, 309 (2018)
132. J. Huang, C. Wang, Z. Liu, X. Qiu, J. Yang, J. Chang, Simultaneouly enhanced durability and performance by employing dopamine copolymerized PEDOT with high work function and water-proofness for inverted perovskite solar cells. J. Mater. Chem. C **6**, 2311 (2018)
133. S. Xu, C. Liu, Z. Xiao, W. Zhong, Y. Luo, H. Ou, J. Wiezorek, Cooperative effect of carbon black and dimethyl sulfoxide on PEDOT:PSS hole transport layer for inverted planar perovskite solar cells. Sol. Energy **157**, 125–132 (2017)
134. D. Huang, T. Goh, J. Kong, Y. Zheng, S. Zhao, Z. Xu, A.D. Taylor, Perovskite solar cells with DMSO-treated PEDOT:PSS holetransport layer exhibit higher photovoltaic performance and enhanced durability. Nanoscale **9**, 4236–4243 (2017)
135. D. Wang, N.K. Elumalai, M.A. Mahmud, M. Wright, M.B. Upama, K.H. Chan, C. Xu, F. Haque, G. Conibeer, A. Uddin, V2O5-PEDOT:PSS bilayer as hole transport layer for highly efficient and stable perovskite solar cells. Org. Electron. **53**, 66–73 (2018)
136. H. Luo, X. Lin, X. Hou, L. Pan, S. Huang, X. Chen, Efficient and air-stable planar perovskite solar cells formed on graphene-oxide-modified PEDOT:PSS hole transport layer. Nano Lett. **9**, 19–29 (2017)
137. W. Sun, Y. Li, Y. Xiao, Z. Zhao, S. Ye, H. Rao, H. Ting, Z. Bian, L. Xiao, C. Huang, Z. Chen, An ammonia modified PEDOT: PSS for interfacial engineering in inverted planar perovskite solar cells. Org. Electron. **46**, 22–27 (2017)
138. C. Zuo, L. Ding, Modified PEDOT layer makes a 1.52 V voc for perovskite/PCBM solar cells. Adv. Energy Mater. **7**, 1601193 (2017)
139. G. Adam, M. Kaltenbrunner, E.D. Glowacki, D.H. Apaydin, M.S. White, H. Heilbrunner, S. Tombe, P. Stadler, B. Ernecker, C.W. Klampfl, N.S. Sariciftci, M.C. Scharber, Solution processed perovskite solar cells using highly conductive PEDOT:PSS interfacial layer. Sol. Energy Mater. Sol. Cells **157**, 318–325 (2016)
140. X. Huang, H. Guo, J. Yang, K. Wang, X. Niu, X. Liu, Moderately reduced graphene oxide/PEDOT:PSS as hole transport layer to fabricate efficient perovskite hybrid solar cells. Org. Electron. **39**, 288–295 (2016)
141. A. Giuri, S.A. Masi, S. Colella, A. Kovtun, S. Dell'Elce, E. Treossi, A. Liscio, C.E. Corcione, A. Rizzo, A. Listorti, Cooperative effect of go and glucose on PEDOT:PSS for high voc and hysteresis-free solution-processed perovskite solar cells. Adv. Funct. Mater. **26**, 6985–6994 (2016)
142. C. Liu, Z. Su, W. Li, F. Jin, B. Chu, J. Wang, H. Zhao, C.S. Lee, J. Tang, B. Kang, Improved performance of perovskite solar cells with a TiO_2/MoO_3 core/shell nanoparticles doped PEDOT:PSS hole-transporter. Org. Electron. **33**, 221–226 (2016)
143. K.M. Reza, A. Gurung, B. Bahrami, S. Mabrouk, H. Elbohy, R. Pathak, K. Chen, A.H. Chowdhury, M.T. Rahman, S. Letourneau, H.-C. Yang, G. Saianand, J.W. Elam, S.B. Darling, Q. Qiao, Tailored PEDOT:PSS hole transport layer for higher performance in perovskite solar cells: Enhancement of electrical and optical properties with improved morphology. J. Energy. Chem. **44**, 41–50 (2020)
144. M. Makha, S.L. Fernandes, S. Jenatsch, T. Offermans, J. Schleuniger, J.-N. Tisserant, A.C. Veron, R. Hany, A transparent, solvent-free laminated top electrode for perovskite solar cells. Sci. Technol. Adv. Mat. **17**, 260–266 (2016)
145. K.M. Kim, S. Ahn, W. Jang, S. Park, O.O. Park, D.H. Wang, Work function optimization of vacuum free top-electrode by PEDOT:PSS/PEI interaction for efficient semi-transparent perovskite solar cells. Sol. Energy Mater. Sol. Cells **176**, 435–440 (2018)